# Identification of oligo(*p*-phenylene vinylene)–naphthalene diimide heterocomplexes by scanning tunneling microscopy and spectroscopy at the liquid–solid interface†

**Inge De Cat,[a] Cornelia Röger,[b] Cameron C. Lee,[c] Freek J. M. Hoeben,[c] Maarten J. Pouderoijen,[c] Albertus P. H. J. Schenning,*[c] Frank Würthner*[b] and Steven De Feyter*[a]**

***Received (in Cambridge, UK) 14th July 2008, Accepted 5th September 2008***
***First published as an Advance Article on the web 7th October 2008***
**DOI: 10.1039/b811961a**

**Co-assembly of a melamine derivative covalently equipped with two oligo(*p*-phenylene vinylene) chromophores and a naphthalene diimide dye results in the formation of heterocomplexes at the liquid–solid interface which was shown using bias dependent imaging and scanning tunneling spectroscopy, despite the disordered nature of the assemblies.**

The autonomous ordering and assembly of molecules on atomically well-defined surfaces is a promising route to make functional surfaces.[1] To increase the functional complexity, often multicomponent structures are targeted.[2] However, identification of multicomponent substrate-supported architectures with molecular to submolecular resolution is not trivial, especially upon lack of long-range order. Here we show that scanning tunneling microscopy (STM) in combination with scanning tunneling spectroscopy (STS) are invaluable tools to reveal the structural and electronic properties of multicomponent assemblies[3] on atomically flat conductive surfaces at the liquid–solid interface, even in complex dynamic and disordered systems.

We have recently shown that oligo(*p*-phenylene vinylene) (OPV) electron donors and perylene diimide (PI) acceptor units can be incorporated in multicomponent donor–acceptor (DA) systems by means of covalent[4] and hydrogen bonds.[5,6] The organization and electronic properties of such systems were studied with STM and STS for covalently bonded systems.[4] For hydrogen-bonded systems, the distortion of PI dyes by bay-substitution, which is necessary to provide sufficient solubility of these pigment colorants, is however disadvantageous for ordered assembly on flat surfaces.[6]

Therefore, in this work PIs were replaced by naphthalene diimide (NI) dyes, which are flat and contain alkyl chains to favor adsorption on highly oriented pyrolytic graphite (HOPG) (Scheme 1).[7] These at core tetraamino-substituted NI dyes were synthesized by nucleophilic substitution of tetrabromo NI **2**, the latter was prepared by condensation of 2,3,6,7-tetrabromonaphthalene dianhydride **1** with ammonium acetate, with the respective alkyl amines (Scheme 1).[8]†

Targeting the formation and electronic characterization of a large 12-membered rosette (Fig. 1) stabilized by 36 hydrogen bonds, the co-assembly of **NI12** and a melamine derivative with two oligo(*p*-phenylene vinylene) chromophores (**(OPV4)$_2$M**)[6] (Fig. 1) was studied with STM and STS at the liquid–solid phenyloctane–graphite interface.

Despite repeated trials in different solvents, none of the pure alkylated naphthalene diimides could be visualized at the liquid–solid interface. In contrast, as reported earlier, **(OPV4)$_2$M** does adsorb forming disordered patterns (Fig. 2a),[6] which can locally evolve into a more ordered arrangement (Fig. 2b). The **(OPV4)$_2$M** molecules appear as bright V-shaped structures. Dimers, trimers and tetramers can be distinguished, which are probably interacting by hydrogen bonding between the melamine units.

After studying the self-assembly of the pure components, a mixture of both **(OPV4)$_2$M** and **NI** was investigated. The best results were obtained with the **NI12** dye bearing the longest alkyl chains. Accordingly the discussion will focus on **(OPV4)$_2$M–NI12** heterocomplexes. STM-images of the 1 : 1 mixture show a highly disordered organization of the molecules (Fig. 2c). These images correspond very well to the ones obtained for pure **(OPV4)$_2$M** despite the fact that **(OPV4)$_2$M** and **NI** form a complex in 1-phenyloctane at the concentration used for the STM experiments.† Even for a large excess of **NI12** (1 : 50) there is still a high degree of disorder (Fig. 2d). However, some new supramolecular structures were formed, in particular a cyclic rosette (Fig. 2e). Since these new patterns

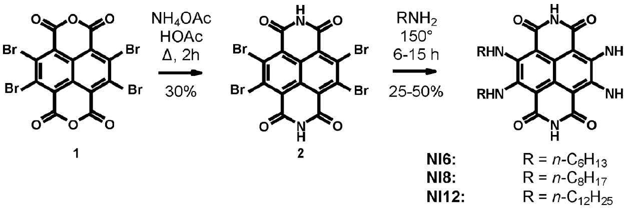

**Scheme 1** Synthesis of tetra-substituted NI colorants.

---

[a] *Department of Chemistry, Division of Molecular and Nanomaterials, Laboratory of Photochemistry and Spectroscopy, and INPAC-Institute for Nanoscale Physics and Chemistry, Katholieke Universiteit Leuven, Celestijnenlaan 200 F, B-3001 Leuven, Belgium. E-mail: Steven.DeFeyter@chem.kuleuven.be*
[b] *Universität Würzburg, Am Hubland, D-97074 Würzburg, Germany. E-mail: wuerthner@chemie.uni-wuerzburg.de*
[c] *Eindhoven University of Technology, P.O. Box 513 MB Eindhoven The Netherlands. E-mail: a.p.h.j.schenning@tue.nl*

† Electronic supplementary information (ESI) available: Synthesis of the alkylated naphthalene diimides. Details on the STM and STS experiments. Bias dependent imaging of **(OPV4)$_2$M**. Temperature dependent absorption spectra in solution. See DOI: 10.1039/b811961a

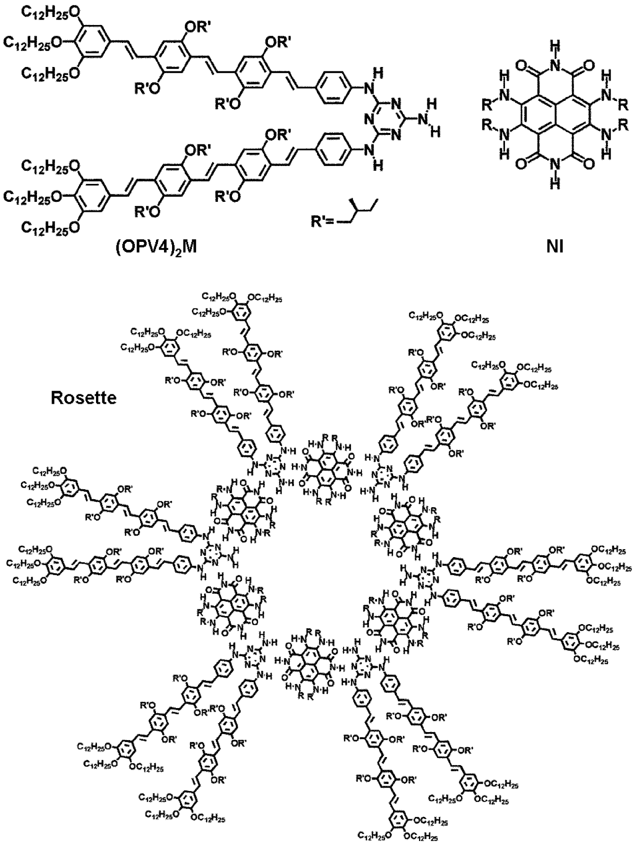

**Fig. 1** Molecular structure of **(OPV4)$_2$M**, **NI12** and the rosette heterocomplex.

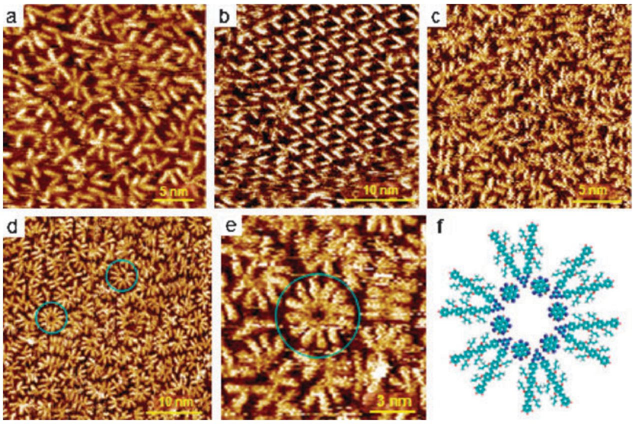

**Fig. 2** STM-images at the 1-phenyloctane–HOPG interface, $I_{\mathrm{set}}$ = 28 pA. (a–b) Pure **(OPV4)$_2$M**. (c) [**(OPV4)$_2$M**] = [**NI12**] = 1.4 mM, $V_{\mathrm{set}}$ = −0.500 V. (d–e) [**(OPV4)$_2$M**] : [**NI12**] = 1 : 50, $V_{\mathrm{set}}$ = −0.800 V. (f) Molecular model of 12-membered rosette.

are only observed when both compounds are present in solution and since the shape of these supramolecular structures is in line with molecular modelling involving both compounds, we can deduce that heterocomplexes were formed. The observed rosette consists of six **(OPV4)$_2$M** molecules, clearly shown in the STM-images. The inner diameter of the rosettes is approximately 2.5 nm and the outer 7.6 nm, which is consistent with a molecular model (Fig. 2f), containing six **(OPV4)$_2$M** and six **NI12** molecules. Because the latter are not seen under these measuring conditions, there is still no direct evidence for the involvement of **NI12** in the supramolecular structures. Therefore, bias dependent imaging and STS-measurements were performed.

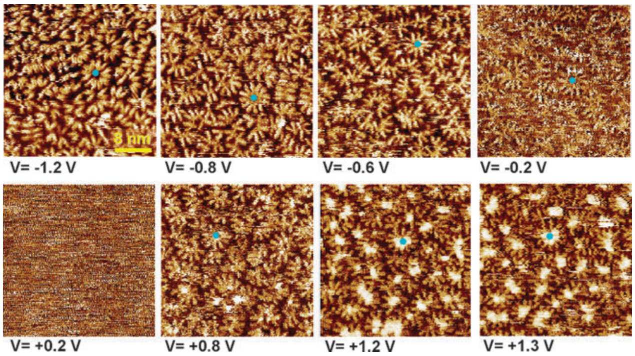

**Fig. 3** Bias dependent imaging of an **(OPV4)$_2$M–NI12** mixture at the 1-phenyloctane–HOPG interface. $I_{\mathrm{set}}$ = 28 pA. A rosette has been highlighted by a blue dot in order to facilitate tracking of the patterns in spite of thermal drift.

With bias dependent imaging, STM-images are obtained sequentially at the same location, while the value of the bias is changed. In this case, the sample bias ($V_{\mathrm{set}}$) was changed from highly negative (−1.2 V) to highly positive (+1.3 V). Fig. 3 shows sequential STM-images at different bias. A rosette has been highlighted by a blue dot in order to facilitate tracking of the patterns in spite of thermal drift. For the STM-images recorded at negative sample bias, the OPV-units appeared very bright and no **NI12** molecules were visible. When the sample bias went to zero, the OPV-units became relatively less bright until they disappeared; the **NI12** molecules were still not detectable. At positive sample bias, not only the OPV-units were visible, but also some bright spots appeared, which are always located in the vicinity of the melamine groups. As bias dependent imaging of pure **(OPV4)$_2$M** does not show such features,† these characteristic white spots are associated with the **NI12** molecules. A linear correlation between the area of the bright spots, *i.e.* the number of **NI12** molecules, and the number of OPV-units (Fig. 4), supports the existence of specific interactions between **NI12** and **(OPV4)$_2$M** molecules, *i.e. via* hydrogen bonding. However, the exact number of **NI12** molecules could not be deduced.†

The dependence of the contrast in the STM-images on the bias can be explained by the electronic properties of the

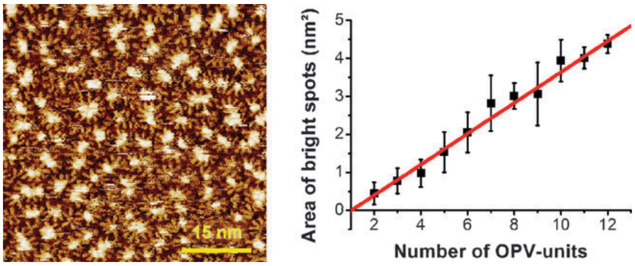

**Fig. 4** Left: STM-image at the 1-phenyloctane–HOPG interface. $I_{\mathrm{set}}$ = 28 pA, $V_{\mathrm{set}}$ = +1.3 V; right: linear correlation between the area of bright spots and the number of OPV-units (combined analysis of 110 structures).

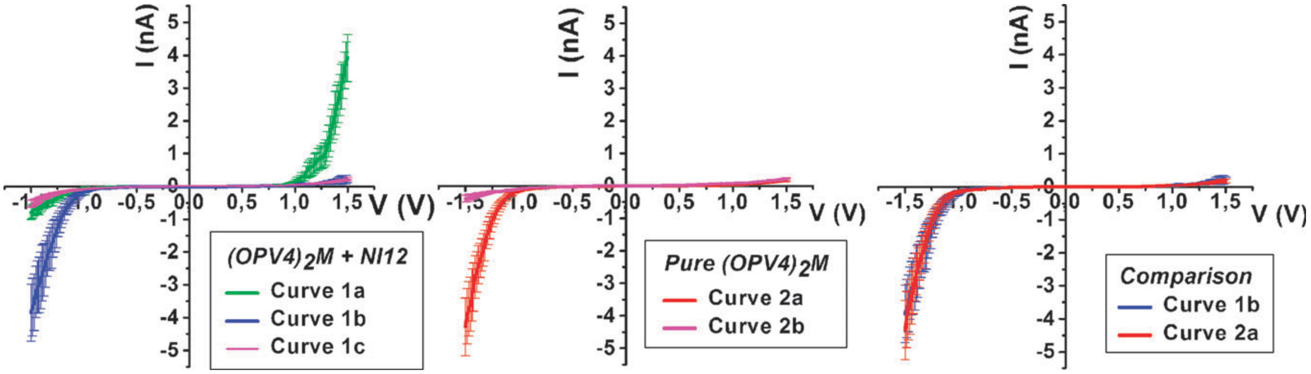

**Fig. 5** STS-measurements of the mixture of **$(OPV4)_2M$** and **NI12** (curve 1a (average of 26 curves), curve 1b (average of 81 curves) and curve 1c (average of 35 curves), $I_{set}$ = 33 pA), STS-measurements of the pure **$(OPV4)_2M$** (curve 2a (average of 78 curves), curve 2b (average of 27 curves, $I_{set}$ = 39 pA) and comparison of the similar curves (1b and 2a). The standard deviation of the averaged STS curves is also indicated.

molecules. At high negative sample bias, the OPV-units appear very bright since the HOMO level is located close to the Fermi level of graphite.[4] Therefore, electrons tunneling from graphite to the tip couple stronger to the HOMO level than to the other energy levels. At high positive sample bias with tunneling electrons from tip to sample, the **NI12** molecules appear very bright, and the tunneling process is likely to be affected by the lowest unoccupied molecular orbital (LUMO). To confirm these results, STS-measurements were carried out.

STS is a powerful experimental technique that probes the electronic properties of the surface. The tip is stopped on a sample coordinate of choice, the feedback-loop which controls the distance between tip and sample according to a given tunneling current setpoint ($I_{set}$) is deactivated and a current–voltage (*IV*) curve is recorded.† These measurements were complicated due to the unstable organization of the molecules on the surface. Therefore, a large amount of *IV*-curves were recorded (different samples, sessions, tips) in random spots on the covered substrate. Since the *IV*-curves showed very distinct characteristics, it was possible to divide them into four categories.† Only three categories are shown in Fig. 5 as the fourth category is the sum (combination) of curve 1a and curve 1b.† Curves 1a and 1b have opposite characteristics: curve 1a shows a high tunneling current for high positive bias, while curve 1b shows a high tunneling current for high negative bias. Curve 1c has a low tunneling current for both negative and positive bias. This curve corresponds most likely to the alkyl chains.[4] To determine the characteristic curves for the conjugated units of **$(OPV4)_2M$** and **NI12**, STS-measurements were performed on a monolayer of pure **$(OPV4)_2M$**. Two types of curves were obtained (Fig. 5, curve 2a and 2b). Curve 2a strongly resembles curve 1b, while curve 2b corresponds to the alkyl chains. Now it can be concluded with certainty that curve 1a and curve 1b correspond to the conjugated units of **NI12** and **$(OPV4)_2M$**, respectively.

The results acquired with STS are consistent with the STM-measurements and bias depending imaging. The electron acceptor **NI12** was only visualized at positive bias and its *IV*-curve (curve 1a) showed a high tunneling current for positive bias, while the tunneling current for negative bias was almost zero. The electron donor **$(OPV4)_2M$**, on the other hand, was most clearly visualized at negative bias and its *IV*-curve confirmed this by showing a high tunneling current for negative bias and a much lower tunneling current for positive bias.

Although no crystalline domains of rosettes were formed and disorder remained, STM was able to resolve these quasi-crystalline[9] monolayers while bias dependent imaging and STS gave more insight into the composition and electronic properties of the supramolecular structures. The origin of monolayer disorder and remedies to improve it are the subject of ongoing studies.

## Notes and references

1 J. V. Barth, G. Costantini and K. Kern, *Nature*, 2005, **437**, 671; R. Madueno, M. T. Räisänen, C. Silien and M. Buck, *Nature*, 2008, **454**, 618; M. In't Veld, P. Iavicoli, S. Haq, D. B. Amabilino and R. Raval, *Chem. Commun.*, 2008, 1536.
2 J. A. Theobald, N. S. Oxtoby, M. A. Phillips, N. R. Champness and P. H. Beton, *Nature*, 2003, **424**, 1029; K. G. Nath, O. Ivasenko, J. A. Miwa, H. Dang, J. D. Wuest, A. Nanci, D. F. Perepichka and F. Rosei, *J. Am. Chem. Soc.*, 2006, **128**, 4212.
3 F. Jäckel, M. D. Watson, K. Müllen and J. P. Rabe, *Phys. Rev. Lett.*, 2004, **92**, 188303; K. Müllen and J. P. Rabe, *Acc. Chem. Res.*, 2008, **41**, 511; S. B. Lei and S. De Feyter, *Top. Curr. Chem.*, 2008, **285**, 269.
4 A. Miura, Z. Chen, H. Uji-i, S. De Feyter, M. Zdanowska, P. Jonkheijm, A. P. H. J. Schenning, E. W. Meijer, F. Würthner and F. C. De Schryver, *J. Am. Chem. Soc.*, 2003, **125**, 14968; H. Uji-i, A. Miura, A. P. H. J. Schenning, E. W. Meijer, Z. Chen, F. Würthner, F. C. De Schryver, M. Van der Auweraer and S. De Feyter, *ChemPhysChem*, 2005, **6**, 2389.
5 F. Würthner, Z. Chen, F. J. M. Hoeben, P. Osswald, C.-C. You, P. Jonkheijm, J. van Herrikhuyzen, A. P. H. J. Schenning, P. P. A. M. van der Schoot, E. W. Meijer, E. H. A. Beckers, S. C. J. Meskers and R. A. J. Janssen, *J. Am. Chem. Soc.*, 2004, **126**, 10611.
6 F. J. M. Hoeben, J. Zhang, C. C. Lee, M. J. Pouderoijen, M. Wolffs, F. Würthner, A. P. H. J. Schenning, E. W. Meijer and S. De Feyter, *Chem.–Eur. J.*, 2008, **14**, 8579.
7 Recent reviews on NI colorants: S. V. Bhosale, C. H. Jani and S. J. Langford, *Chem. Soc. Rev.*, 2008, **37**, 331; S. Bhosale, S. A. L. Sisson, N. Sakai and S. Matile, *Org. Biomol. Chem.*, 2006, **4**, 3031.
8 C. Röger and F. Würthner, *J. Org. Chem.*, 2007, **72**, 8070.
9 R. Otero, M. Lukas, R. E. A. Kelly, W. Xu, E. Lægsgaard, I. Stensgaard, L. N. Kantorovich and F. Besenbacher, *Science*, 2008, **319**, 313.